Philosophical Magazine Letters,
Vol. 86, No. 7, July 2006, 435–441

Taylor & Francis
Taylor & Francis Group

Anisotropic compressive properties of iron subjected to single-pass equal-channel angular pressing

W. Z. HAN*†, Z. F. ZHANG†,
S. D. WU*†, S. X. LI† and Y. D. WANG‡

†Shenyang National Laboratory for Materials Science,
Institute of Metal Research, Chinese Academy of Science,
Shenyang 110016, China
‡Department of Materials Science and Engineering,
Northeastern University, Shenyang 110014, China

(*Received 15 March 2006; in final form 2 June 2006*)

The anisotropic compressive properties and shear deformation mechanism of iron subjected to equal-channel angular pressing (ECAP) with single-pass have been investigated. It was found that the anisotropic compressive properties can be attributed to the effect of the ECAP shear plane. It is suggested that the ECAP shear plane induced by the first pass of ECAP is a relatively weak plane in terms of resisting subsequent shear deformation.

1. Introduction

Equal-channel angular pressing (ECAP) has been demonstrated to be an effective technique for producing truly bulk, fully dense and contamination-free metals with grains ranging from submicrometre to even nanometre sizes [1, 2]. In terms of mechanical behaviour, ultrafine-grained materials exhibit relatively high hardness, improved compressive and tensile strengths, but deteriorated ductility compared with their coarse-grained counterparts [3, 4].

Figure 1a demonstrates the schematic drawing for an ECAP die. As a work-piece is pressed through an ECAP die, it is generally accepted that the large shear deformation always occurs along the intersection plane between the entrance and exit channels, and the intersection plane is just the shear deformation plane. Based on this consideration, Segal [5] and Agnew *et al*. [6] designed some experiments to investigate the influence of the shear plane on the mechanical properties of iron and Mg alloy subjected to ECAP. However, many experiments have proved that, after pressing for the first pass, the shape of the billet will be changed and a group of shear flow lines will be formed in the deformed billet, as shown in figures 1b and c. The angle between shear flow lines and the extrusion direction is defined as shear angle θ_S,

*Corresponding author. Email: wzhan@imr.ac.cn and shdwu@imr.ac.cn

Philosophical Magazine Letters
ISSN 0950-0839 print/ISSN 1362-3036 online © 2006 Taylor & Francis
http://www.tandf.co.uk/journals
DOI: 10.1080/09500830600847095

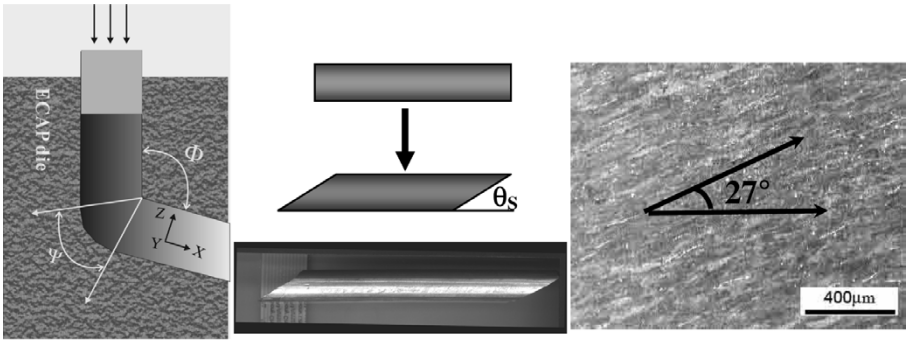

Figure 1. (a) Schematic illustration of ECAP die; (b) state of the billet before and after ECAP; (c) SEM–ECC photograph for the shear flow lines on the y-plane.

which can be calculated by [7–9]:

$$\theta_S = \operatorname{arc\,cot}\left[2\cot\left(\frac{\phi}{2}+\frac{\psi}{2}\right)+\psi\operatorname{cosec}\left(\frac{\phi}{2}+\frac{\psi}{2}\right)\right], \tag{1}$$

where ϕ is the channel angle and ψ is the angle of the circular joint between the tubes at the left corner region, as shown in figure 1a. It indicates that the geometrical shape of the ECAP die decides the value of shear angle, θ_S. For an ECAP die with $\phi = 90^\circ$ and $\psi = 0^\circ$, the shear angle θ_S is 26.6°, which is consistent with many experimental results [10–12]. Hereafter, the shear plane along the flow line direction is named as the ECAP shear plane, which differs from the general shear deformation plane [5]. The shear flow lines formed during ECAP may lead to anisotropy in the mechanical properties. However, there are few reports considering this. Recently, Fang *et al.* [13] found that the fracture plane of Al–Cu alloy 'ECAPed' with single pass is approximately parallel to the ECAP shear plane. It is obvious that the ECAP shear plane along the flow line direction plays an important role in the deformation and fracture of ECAPed materials. In the present work, we attempt systematically to reveal the anistropic compressive properties of single-pass ECAPed iron specimens using different orientations with respect to the ECAP shear plane to obtain a better understanding of the deformation mechanism.

2. Experimental procedures

Samples of commercial Armco iron (99.3% purity) with an average grain size of ~100 μm were extruded for one pass at room temperature. The tooling parameters of the die used for the ECAP were $\phi = 90^\circ$ and $\psi = 0^\circ$; the cross-section of the work piece was 10 mm in diameter. Compression test specimens with a dimension of $3 \times 3 \times 6$ mm were cut from the extruded billets. Figure 2 illustrates the compression specimens having different orientations with respect to the ECAP shear plane,

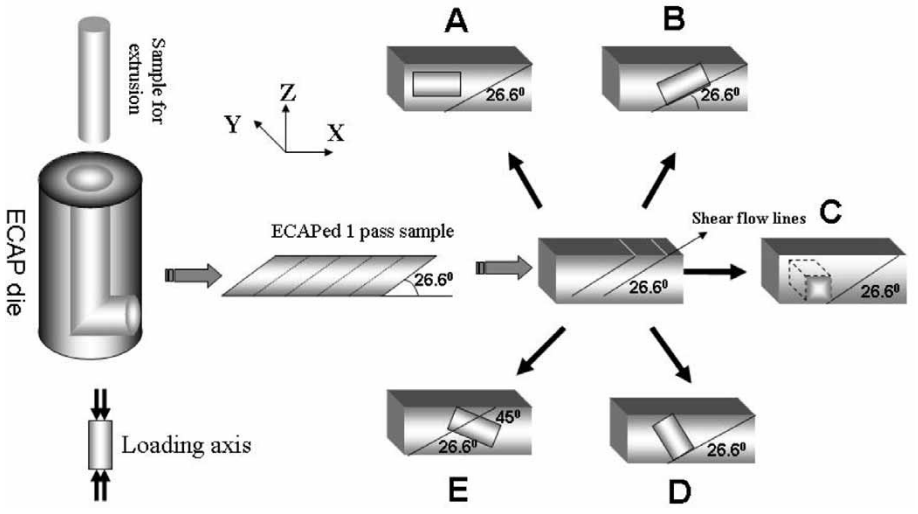

Figure 2. Schematic illustrations of the specially designed compressive specimens.

denoted as A, B, C, D and E, respectively. Quasi-static compression tests at a strain rate of $1 \times 10^{-4}\,s^{-1}$ were performed on a MTS 810 machine. To observe the surface deformation features, the side surfaces of the specimens were polished to a mirror finish before compression.

3. Results and discussion

Figure 3 presents the engineering stress–strain curves for the five specimens. The ultimate compressive strength σ_U is taken from the plateau stress in the stress–strain curve. It can be seen that the values of σ_U for different specimens span a wide range from 550 to 710 MPa. Specimen A has the most common orientation verified by many experiments. Its compressive strength σ_U is 600 MPa, comparable with the datum in the literature [11]. Specimen E was specially designed to make its ECAP shear plane at an angle of 45° with respect to the loading axis. It is apparent that specimen E has the lowest compressive strength among the five specimens. A feature of specimen C is that its loading axis is along the *y*-direction, as shown in figure 2; it has the highest strength ($\sigma_U = 710$ MPa). The compressive strengths of specimens B and D are 650 and 660 MPa, respectively. The two specimens display a quite similar compressive strength, even though they have totally different orientations. The above results indicate that iron subjected to one-pass ECAP would display an obvious anisotropy in compressive strength.

The surface deformation features of these compressive specimens are shown in figures 4a–e. It can be seen that the macro-scale shear bands in specimens A–E are orientated at different angles with respect to the loading direction. For specimen A, the shear bands are not along the maximum shear stress plane, but mainly along the

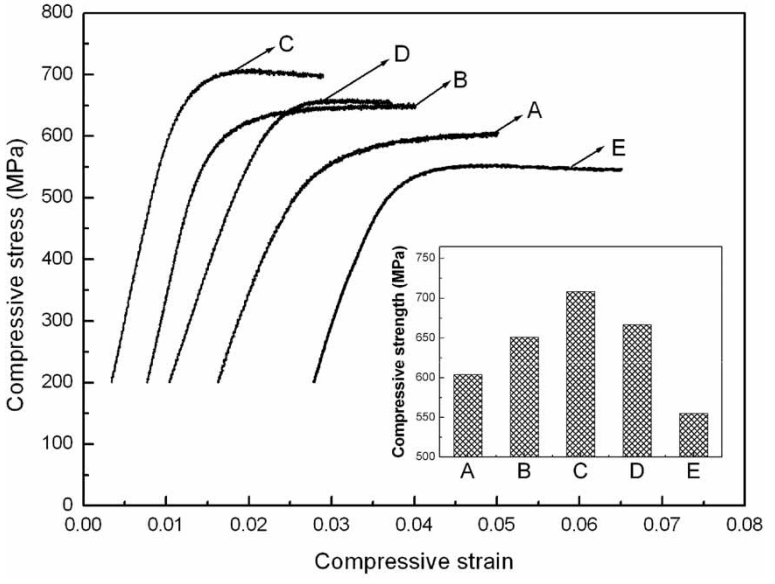

Figure 3. Typical engineering strain–stress curves for specimens A, B, C, D and E. The inset shows the compressive strengths of the specimens.

ECAP shear plane, which developed during ECAP (as verified by an SEM–ECC image). As shown in figure 4a, the compressive angle θ_C is about 27° for specimen A, and equals the designed angle θ_D. It is demonstrated that shear deformation still takes place on the ECAP shear plane even though it deviates from the maximum shear stress plane. Different deformation features are observed in specimens B, C and D, as shown in figures 4b, c. Their values of θ_C are around 45° and the macro-scale shear bands are approximately along the maximum shear stress plane, but not along the ECAP shear plane. The ECAP shear planes in specimens B–D are parallel or vertical to the loading axis, making it difficult to form shear bands during deformation. The deformation feature of specimen E is, to some extent, similar to that in specimen A – their shear bands are along the ECAP shear plane at an angle of 45° with respect to the compressive axis. On the neighbouring side surface of specimens A–E, the macro-scale shear traces are vertical to the loading axis.

Comparing the compressive anisotropy with the deformation features, it is possible to establish a quantitative relation between shear bands and compressive strength. According to the relation between σ_U and τ_S on the shear plane:

$$\tau_S = \sigma_U \sin(\theta_C)\cos(\theta_C) \tag{2}$$

one can calculate that the shear stress (τ_S) of specimens A and E are 243 and 275 MPa, respectively. However, the critical shear stress of specimens A and E should be the same because their deformation occurs only on the ECAP shear plane. The above results indicate that the difference in shear stresses may arise from overlooking the effect of the normal stress σ_S on the shear plane:

$$\sigma_S = \sigma_U \sin(\theta_C)\sin(\theta_C) \tag{3}$$

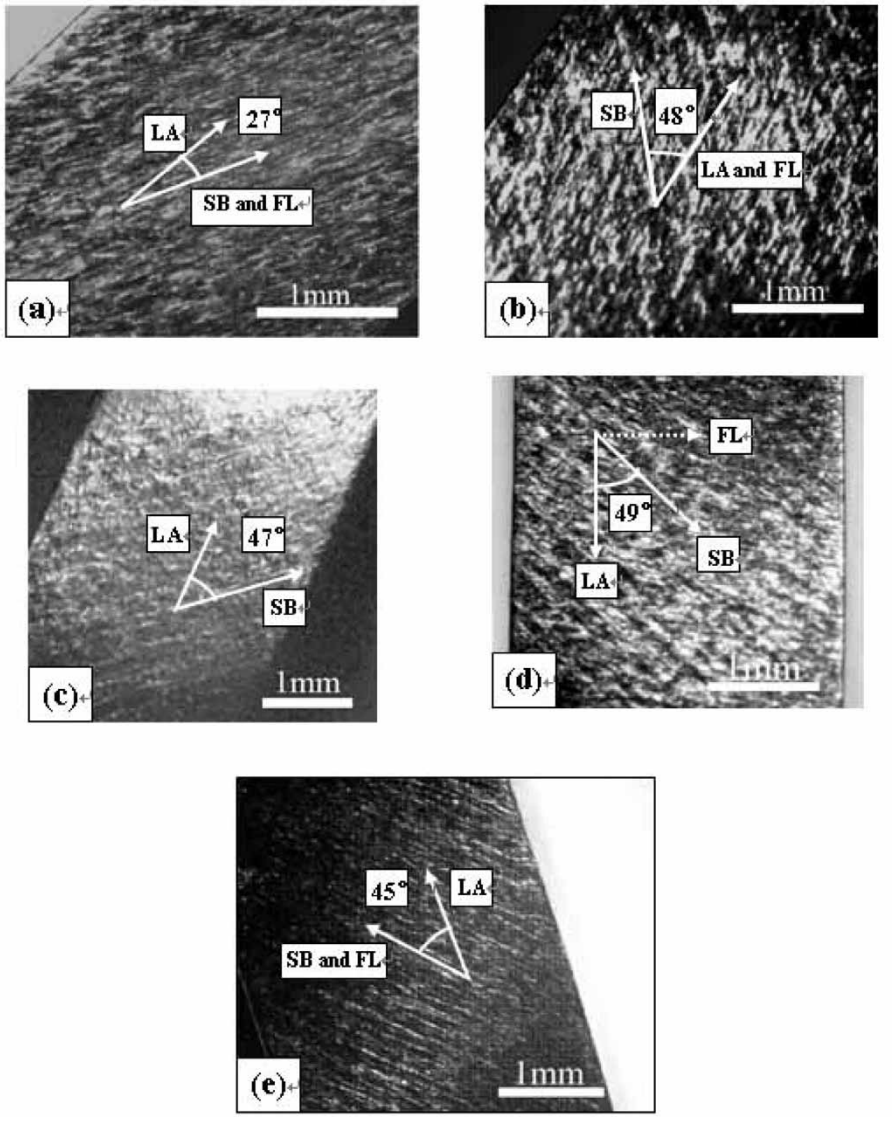

Figure 4. Deformation morphology of (a) specimen A, (b) specimen B, (c) specimen C, (d) specimen D, and (e) specimen E. LA, loading axis; SB, shear bands; FL, flow lines.

For a better understanding of the relationship between the ultimate compressive strength σ_U and the macro-scale shear bands, we use the Mohr–Coulomb criterion, which is generally applied to high-strength materials (BMG or ultrafine-grained materials) [14, 15]. According to this criterion, when a specimen is subjected to a normal compressive stress, σ_S, the shear stress on the shear plane, τ_S, can be expressed as:

$$\tau_S = \tau_0 + \mu\sigma_S \tag{4}$$

Table 1. Mechanical properties of the five specimens.

	Specimen				
	A	B	C	D	E
θ_D (degree)	26.6	0	0	90	45
θ_C (degree)	27	48	47	49	45
σ_U (MPa)	600	650	710	660	550
τ_S (MPa)	243	323	354	327	275
τ_0 (MPa)	217	247	274	247	217

The angle between the shear flow lines and the loading axis is the design angle θ_D; the angle between the macro-shear band and the loading axis is the compressive angle θ_C; σ_U stands for the ultimate compressive strength, τ_S the shear stress on the actual shear plane and τ_0 the critical shear stress.

where μ is a constant for the ultrafine-grained iron, and τ_0 is the critical shear stress of the shear plane without normal stress. For specimens A and E, deformation takes place mostly on the ECAP shear plane and, therefore, the value of τ_0 should be almost identical. Substituting the two values of σ_S and τ_S into equation (4), the constant μ and the critical shear stress τ_0 can be expressed as:

$$\mu = \frac{\tau_S^A - \tau_S^E}{\sigma_S^A - \sigma_S^E} = 0.212 \tag{5}$$

and

$$\tau_0^A = \tau_0^E = \tau_S^A - \mu\sigma_S^A = 217\,\text{MPa}. \tag{6}$$

According to equation (4) and with the constant $\mu = 0.212$, one can also calculate the critical shear stress τ_0 for specimens B, C and D, as listed in table 1. The above results indicate that the value of τ_0 for the ECAP shear plane is the lowest amongst the various kinds of shear planes. This is reasonable because the direction of the shear flow lines is the same as the grain elongation direction (the average aspect ratio of the elongated grains is 2.77) [5, 16], along with the free slip distance for dislocation motion, which is larger than that along the other directions. Therefore, it is easier for dislocations to glide, resulting in a weaker ECAP shear plane. For specimens A and E, the compressive angles θ_C^A and θ_C^E are equal to 27° and 45°, respectively; therefore, the ultimate compressive strength of specimen A is slightly higher than that of specimen E. On the other hand, the shear deformation of specimens B, C and D occurs on a new shear plane with relatively high critical resistance stresses, which is different from the ECAP shear plane; hence, the three specimens have higher ultimate strengths than those of specimens A and E. In addition, specimens B and D have the same critical shear stress, resulting in their compressive strengths being similar to each other regardless of whether the ECAP shear plane is located along or vertical to the stress axis. The difference in compressive strengths between specimens B (or D) and C might be associated with the texture. According to the modelling and experimental results of Li *et al.* [17], ⟨111⟩ fibre texture, which parallels the *y*-direction, is formed after ECAP. Specimen

C has the greatest value of ultimate strength amongst the three specimens (B, C and D) because there are ⟨111⟩ fibres texture along the loading axis, which is the hardest direction for bcc iron [18]. Owing to the effects of the ECAP shear plane, materials processed by ECAP with one-pass have an obvious anisotropy in compressive properties.

4. Conclusion

A group of shear flow lines were formed in an iron billet after one-pass ECAP. It is evident that the ECAP shear plane has the lowest value of shear strength to resist shear deformation. Therefore, the ultimate compressive strength of the ECAPed iron displays strong anisotropy, which can be attributed to the effect of the ECAP shear planes.

Acknowledgments

This work was financially supported by Key Project of Fundamental Research of China No. 2004CB619100, the National Natural Sciences Funds of China (CNSF) under grant No. 50371090 and No. 50571102. Z. F. Zhang would like to thank the financial support of 'Hundred of Talents Project' by the Chinese Academy of Sciences.

References

[1] R.Z. Valiev, R.K. Islamgaliev and I.V. Alexandrov, Prog. Mater. Sci. **45** 103 (2000).
[2] T.C. Lowe, R.Z. Valiev (Editors), *Investigations and Applications of Severe Plastic Deformation* (Kluwer, Dordrecht, 2000).
[3] Q. Wei, L. Kecskes, T. Jiao, *et al*., Acta Mater. **52** 1895 (2004).
[4] S.D. Wu, Z.G. Wang, C.B. Jiang, *et al*., Scripta Mater. **48** 1605 (2003).
[5] V.M. Segal, Mater. Sci. Eng. A **197** 157 (1995).
[6] S.R. Agnew, J.A. Horton, T.M. Lillo, *et al*., Scripta Mater. **50** 377 (2004).
[7] Y. Iwahashi, J.T. Wang, *et al*., Scripta Mater. **35** 143 (1996).
[8] M. Furukawa, Y. Iwahashi, Z. Horita, *et al*., Mater. Sci. Eng. A **257** 328 (1998).
[9] M. Furukawa, Z. Horita and T.G. Langdon, Mater. Sci. Eng. A **332** 97 (2002).
[10] Y. Iwahashi, Z. Horita, M. Nemoto, *et al*., Metall. Mater. Trans. A **29** 2245 (1998).
[11] B.Q. Han, E.J. Lavernia and F.A. Mohamed, Metall. Mater. Trans. A **35** 71 (2004).
[12] Y. Fukuda, K. Oh-ishi, M. Furukawa, *et al*., Acta Mater. **52** 1387 (2004).
[13] D.R. Fang, Z.F. Zhang, S.D. Wu, *et al*., Mater. Sci. Eng. A **426** 305 (2006).
[14] Z.F. Zhang, G. He, J. Eckert, *et al*., Phys. Rev. Lett. **91** 045505 (2003).
[15] Z.F. Zhang, J. Eckert and L. Schultz, Acta. Mater. **51** 1167 (2003).
[16] K. Kamachi, M. Furukawa, Z. Horita, *et al*., Mater. Sci. Eng. A **347** 223 (2003).
[17] S.Y. Li, A.A. Gazder, I.J. Beyerlein, *et al*., Acta Mater. **54** 1087 (2006).
[18] E.A. Calnan and J.B. Clews, Phil. Mag. **45** 616 (1951).